Energy, Mines and Resources Canada

Énergie, Mines et Ressources Canada

CANMET

Canada Centre for Mineral and Energy Technology

Centre canadien de la technologie des minéraux et de l'énergie

Mining Research Laboratories

Laboratoires de recherche minière

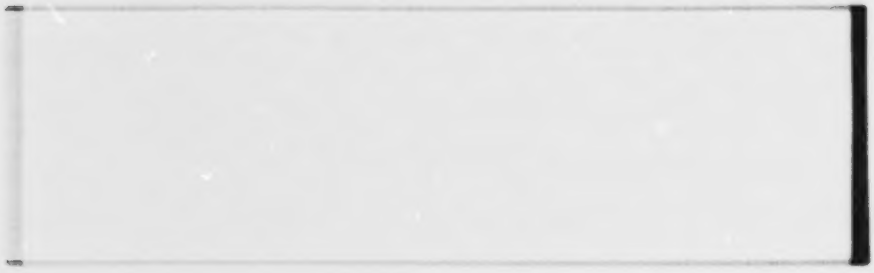

Canada

89-02632/

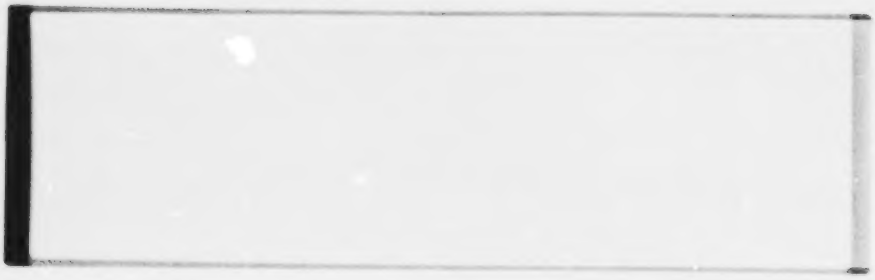

A TECHNICAL NOTE ON THE FORWARD AND BACKWARD THORON PROGENY COLLECTION CHARACTERISTICS OF GRADED WIRE SCREENS

J. Bigu R. Holub and J. Zhou

DIVISIONAL REPORT MRL 88-142 (TR)

MICROMEDIA

This document is an unedited interim report prepared primarily for discussion and internal reporting purposes. It does not represent a final expression of the opinion of the Canadian Centre for Mineral and Energy Technology (CANMET)

30 pp

A TECHNICAL NOTE ON THE FORWARD AND BACKWARD THORON PROGENY COLLECTION CHARACTERISTICS OF GRADED WIRE SCREENS

J. Bigu*. R. Holub** and J. Zhou***

ABSTRACT

A preliminary study has been conducted to determine the thoron progeny size distribution by means of an array of four graded wire screens of different sizes (i.e., mesh No. 40. 80. 250 and 500 per inch). Experiments were conducted in a radon/ thoron test facility of the walk-in type. Tests were also carried out in order to measure two variables which are important in the calculation of radioactive aerosol size distribution by wire screens. namely. the collection efficiency of the screens. and the screen forward-to-backward radioactivity ratio. The majority of the experiments were conducted at moderate aerosol concentrations. i.e., $\geq 6 \times 10^3$ cm^{-3} to $\sim 1.6 \times 10^4$ cm^{-3}. The few experiments that were run at relatively low aerosol concentrations ($\sim 2 \times 10^3$ cm^{-3}) suggest that a low size radioactive particle (thoron progeny) component is present. However. in order to improve sensitivity and particle size resolution. experiments should be conducted at as low an aerosol concentration as possible and using sets of screens of higher mesh numbers. Furthermore. the screens should be of the same. or nearly the same mesh size to maximize their collection efficiency.

Key words: Thoron progeny: Size distribution: Wire screens.

*Research Scientist and Radiation/Respirable Dust/Ventilation Project Leader. Elliot Lake Laboratory. CANMET. Energy. Mines and Resources Canada. Elliot Lake. Ontario. Canada. **Physicist. Denver Research Center. U.S. Bureau of Mines. Denver. CO. ***IAEA Fellow.

NOTE TECHNIQUE SUR LES CARACTÉRISTIQUES DE CAPTAGE AVANT ET ARRIÈRE DES DESCENDANTS RADIOACTIFS DU THORON PAR DES TAMIS EN FIL MÉTALLIQUE CALIBRÉS

J. Bigu*, R. Holub** et J. Zhou***

RÉSUMÉ

Une étude préliminaire a été effectuée en vue de déterminer la distribution granulométrique des descendants radioactifs du thoron au moyen d'un ensemble de quatre tamis en fil métallique calibrés de dimensions différentes (40, 80, 250 et 500 mesh). Les expériences ont été réalisées dans une installation d'essai du radon/thoron de type penderie. Des essais ont aussi été effectués en vue de mesurer deux variables importantes dans le calcul de la distribution granulométrique d'aérosols radioactifs au moyen de tamis en fil métallique, soit le rendement de captage des tamis et le rapport de radioactivité avant et arrière des tamis. Dans la plus grande partie des expériences les concentrations des aérosols étaient moyennes, c.-à-d. comprises entre 6×10^3 cm^{-3} et environ $1,6 \times 10^4$ cm^{-3}. Les quelques expériences réalisées à des concentrations d'aérosols relativement faibles (environ 2×10^3 cm^{-3}) portent à croire qu'une substance radioactive (descendant du radon) sous forme de particules de petite taille est présente. Cependant, pour améliorer la sensibilité et la résolution de la taille des particules, des expériences devraient être effectuées à une concentration d'aérosol aussi faible que possible, avec des ensembles de tamis ayant des nombres de mailles par pouce linéaire plus élevés. De plus, pour que leur rendement de captage soit maximal, les tamis devraient avoir la même, ou pratiquement la même, ouverture de maille.

Mots-clés : descendants radioactifs du thoron, distribution granulométrique, tamis en fil métallique.

*Chercheur scientifique et chef de projet en matière de rayonnements/poussières inhalables/ventilation, Laboratoire d'Elliot Lake, CANMET, Énergie, Mines et Ressources Canada, Elliot Lake (Ontario), Canada. **Physicien, Denver Research Center, U.S. Bureau of Mines, Denver (Col.). ***Membre de L'AIEA.

CONTENTS

	Page
ABSTRACT	i
RESUME	ii
INTRODUCTION	1
EXPERIMENTAL PROCEDURE	2
BACKGROUND INFORMATION AND DEFINITIONS	5
EXPERIMENTAL RESULTS AND DISCUSSION	7
REFERENCES	10

TABLES

No.		
1.	Screen characteristics	12
2.	Average thoron progeny and aerosol conditions in the RTTF	13
3.	Thoron progeny losses on wire screens	14
4.	Thoron progeny losses on wire screens	15
5.	Thoron progeny losses on wire screens	17
6.	Thoron progeny forward to backward ratios for several wire screens.	21

FIGURES

1.	Size distributions (aerosol concentration and particle volume) corresponding to the aerosol cloud in the RTTF	22
2.	Size distributions (aerosol concentration and particle volume) corresponding to the aerosol cloud (NaCl) in the RTTF	23
3.	dA/Adlog D_p versus particle size for WL(Tn) and ^{212}Pb	24
4.	dA/AdlogD_p versus particle size for WL(Tn) corresponding to two different experiments at low aerosol concentration conditions	25
5.	dA/AdlogD_p versus particle size for ^{212}Bi, ^{212}Pb and WL(Tn) at low aerosol concentration conditions	26

INTRODUCTION

The short-lived decay products of radon and thoron are usually found attached to airborne particles which are present in virtually any atmosphere. A small fraction of these decay products can be found, however, in an unattached state as neutral atoms or electrically charged particles (ions). It should be noted that in reality unattached particles usually consist of, say, a ^{218}Po atom or ion surrounded by a few dozen molecules of condensible species present in most atmospheres.

The size distribution and diffusion coefficients of radon and thoron progeny are important variables as they largely determine the deposition characteristics in the respiratory system, and hence the health effects associated with the inhalation of these radioactive decay products.

The diffusion coefficients of radioactive aerosols such as ^{218}Po and ^{212}Pb have been measured by several authors (1-4). Thorough measurements have made it clear that particle size and diffusion coefficients are usually multi-valued (3,5).

The size properties of unattached ^{218}Po clusters using multiple screen techniques have been investigated by Holub and Knutson (5). In 1987, a collaborative effort between the U.S. Bureau of Mines (Denver Research Center) and the Elliot Lake Laboratory (CANMET, EMR) was initiated in order to use the same technique to investigate the size properties of thoron progeny under laboratory controlled conditions and in underground uranium mines in the Elliot Lake area.

An important parameter required for the analysis of multiple screen data is the collection efficiency of the screens. Hence, it is of interest to determine: 1) the amount of a given radioisotope that deposits on the screens, and 2) the deposition pattern of the radioisotope around the wires of

the screen.

This report presents data regarding the above. More specifically, data pertaining to front-to-back thoron progeny activity on the screens as well as some preliminary thoron progeny size distributions are given. The experimental data were obtained under laboratory controlled conditions in a Radon/Thoron Test Facility of the walk-in type.

EXPERIMENTAL PROCEDURE

Screen 'batteries' were exposed to thoron progeny atmospheres in a Radon/Thoron Test Facility (RTTF) of the walk-in type. Each battery consisted of 4 screens of different Tyler mesh number, namely numbers 40, 80, 250 and 500. The screens were mounted on brass rings 1 mm thick and the entire stack loaded into adapted filter holders.

Three screen battery configurations were used:

1. Screens were mounted from the finest size (No. 500) facing the airflow to the coarsest size (No. 40) at the end, i.e., 500, 250, 80 and 40;
2. Screens were mounted from the coarsest size (No. 40) facing the airflow to the finest size (No. 500) at the back of the battery, i.e., 40, 80, 250 and 500 (configuration A);
3. Screens were mounted in the same order as that indicated in item 2, but the side of the screen facing the airflow was reversed (configuration B).

Thoron progeny α-particle activity was counted according to standard techniques using ZnS(Ag) screen/photomultiplier scalers. Thoron progeny concentrations in the RTTF and on the screens were determined using a two gross α-count method described elsewhere (6). The method consists of two 15 min α-particle counts, 2 min and 102 min after the end of a 10 min sampling period. Furthermore, additional 10 min or 30 min α-particle counts were taken between or after the above two α-particle counts, respectively, in order to

follow the growth and decay of α-particle activity on the screens. These additional α-particle counts were also used to calculate the forward-to-backward α-particle activity ratio on the screens. i.e.. F/B for short. see below.

Screen configurations A and B were used to determine F/B by exposing them in sequence for a 10 min period (see above). to the same controlled thoron progeny atmosphere. as follows. Alpha-particle activity measurements on screens mounted according to configuration A were carried out with the exposed side of the screen (i.e.. side facing the air stream) facing the nuclear detector. For screens mounted according to configuration B. the exposed side of the screen was reversed after exposure and the 'unexposed' side was counted.

The exposure and measurement of screens mounted according to configurations A and B can also be summarized as follows:

1. Configuration A. "Right" side out exposure followed by right side out activity measurement.
2. Configuration B. "Wrong" side out exposure followed by right side out activity measurement.

It should be noted that right side out exposure followed by wrong side out measurement is equivalent to item 2. However. this procedure would involve a change in source-detector geometry because of the brass ring. and is. therefore. not used here. The terminology. right side out and wrong side out. is used in this report to indicate the side of the screen/brass ring configuration facing the air stream. i.e..

Right side out: air stream entering the screen first followed by the brass ring (configuration A):

Wrong side out: air stream entering the brass ring first followed by the screen (configuration B).

As indicated above, the ratio F/B permits the calculation of the collection efficiency of the screens for the radon and thoron progenies.

Thoron progeny atmospheres were produced by injecting thoron gas (^{220}Rn) into the RTTF by means of a ^{228}Th dry-source of the flow-through type model Tn-1250 manufactured by Pylon Electronic Development (Ottawa, Canada).

The air concentration of ^{212}Pb, ^{212}Bi, and the thoron progeny Working Level, i.e., $[^{212}Pb]$, $[^{212}Bi]$ and WL(Tn), respectively, were measured during operation of the RTTF. In addition, the temperature (T) and the relative humidity (RH) in the RTTF were noted.

The thoron progeny Working Level, WL(Tn), $[^{212}Pb]$ and $[^{212}Bi]$ were adjusted to several levels according to experimental needs by varying the aerosol concentration, N, in the RTTF. The aerosol concentration was, in turn, adjusted to vary the thoron progeny unattached fraction. The aerosol concentration was routinely monitored using a condensation nuclei counter model Rich 200 manufactured by Environment One (U.S.A.). It should be noted that in the context of this paper, the term, aerosol concentration, is used to indicate condensation nuclei (CN) concentration as opposed to radioactive aerosol concentrations.

Aerosols were produced using variable concentrations of NaCl in aqueous solutions by means of an atomizer model 3076 in conjunction with an air supply system, desiccator and charge neutralizer, all manufactured by TSI (U.S.A.).

Aerosol size distribution in the RTTF was determined using a Differential Mobility Particle Sizer (DMPS) model 3932 in conjunction with a condensation nuclei counter, model 3020, both manufactured by TSI.

The characteristics of the wire screens are given in Table 1. The range of environmental conditions under which the experiments were conducted is shown in Table 2.

BACKGROUND INFORMATION AND DEFINITIONS

When a wire screen is exposed to a stream of radon progeny or thoron progeny, the unattached short-lived decay products of radon and thoron 'attach' themselves readily to the surface of the wires in the screen. The extent of this attachment or deposition depends on the physical and geometrical characteristics of the screens (5).

Little is known about the distribution of these radioisotopes around the wire. However, when an exposed wire screen is examined, α-particle activity on the front of the screen as well as on the back of the screen is measured. Furthermore, the ratio of α-particle activity measured on the front of the screen (forward activity) to the α-particle activity measured on the back of the screen (backward activity) is known to depend on the characteristics of the wire screen such as number of wires per unit of length and diameter of the wire. The above ratio is commonly referred to as the forward (F) to backward (B) activity ratio or F/B, for short.

Because of the unknown distribution of radon (thoron) progeny around the wires, it should not be surprising if some of this radioactivity is not detected by either forward or backward α-activity measurements. Hence, losses of activity on the screen, or screen losses (SL), for short, should be taken into consideration.

Since measurements of α-particle activity using wire screens depend on the efficiency of the screen in collecting radon (thoron) progeny, F/B and SL should be known accurately. If the ratio F/B and SL are known, the efficiency of a screen can be determined by measuring the forward activity (F) only. Calling F/B = a, it is easy to show that the total, i.e., true or corrected, T, α-count on a screen is given by:

$$T = \left(\frac{1+a}{a}\right) F(1+SL) \qquad \text{Eq 1}$$

If a battery of screens of different sizes is used to determine, say, diffusion coefficient spectra, the ratio F/B for each screen should be determined using the battery arrangement (assembly) and not each screen independently.

There are two different ways to determine the F/B ratios of the different screens in a battery assembly, namely:

1. Simultaneous exposure of two identical sets of battery screens followed by simultaneous measurement of the activity deposited on each screen; and
2. Two identical sets of battery screens are exposed, and measured, sequentially.

In both cases, one set of battery screens is used to measure the forward activity, whereas the other is used to determine the backward activity. The data presented here have been obtained following method 2. In each exposure, a screen battery consisting of 4 different screens (40, 80, 250 and 500) and a back filter (BF), as the last stage of the battery, is exposed concurrently with a reference filter holder/filter assembly to collect all the activity. The difference in activity between the battery and the reference filter gives a measure of the screen losses as indicated below.

An 'absolute' screen loss can be defined for the radioactive variable A (where in our case A can be ^{212}Pb, ^{212}Bi, or WL(Tn) as follows:

$$SL(A) = A_a - (\Sigma_s A_{s,f} + \Sigma_s A_{s,b} + \bar{A}_{BF}) \qquad \text{Eq 2}$$

where, SL(A) is the screen loss for radiation variable A, i.e., ^{212}Pb, ^{212}Bi or WL(Tn)

A_a is the measured variable A in air using the reference filter

$A_{s,f}$ is the variable A on the screen as measured in the forward configuration. The symbol Σ_s indicates summation over all the screens making up the battery

$A_{s,b}$ is the same as $A_{s,f}$ except that it refers to the backward

configuration.

$\bar{A}_{BF}$ is the variable A measured on the battery backfilter. The horizontal bar indicates the average value of A_{BF} for the batteries in the forward and backward measurement configuration.

A relative screen loss coefficient, RSL, can be defined as follows:

$$RSL(A) = SL(A)/A_a \qquad \text{Eq 3}$$

When the unattached radon (thoron) progeny fraction is small, i.e., for relatively high aerosol concentrations, the following inequality is true:

$$\bar{A}_{BF} >> \Sigma_s A_{s,f} - \Sigma_s A_{s,b} \qquad \text{Eq 4}$$

Hence, $\bar{A}_{BF} \simeq A_a$, and Equation 2 can be simplified:

$$SL(A) \simeq \Sigma_s A_{f,b} \qquad \text{Eq 5}$$

where $\Sigma_s A_{f,b}$ is the short form for the right hand side of Equation 4. Consequently:

$$RSL(A) \sim (\Sigma_s A_{f,b})/\bar{A}_{BF} \qquad \text{Eq 6}$$

Equation 6 applies to most cases presented here because of the relatively high aerosol concentration, N, used. For cases where the unattached fraction is high, i.e., very low N, Equations 2 and 3 should be used.

EXPERIMENTAL RESULTS AND DISCUSSION

A summary of the results obtained is shown in Tables 2 to 6 and Figures 1 to 5. Table 2 shows thoron progeny concentration and aerosol concentration conditions in the RTTF under which experiments were conducted. The range of values measured are as follows: aerosol concentration $N = 1.9 \times 10^3 - 1.6 \times 10^4$ cm^{-3}; $WL(Tn) = 0.5 - 16$; $[^{212}Bi]/[^{212}Pb] = 0.4 - 0.5$. Tables 3 to 5 show the screen radioactivity losses as defined by Equations 5 and 6. Table 6 shows the forward to backward radioactivity ratio F/B.

The data of Tables 4 and 5 show that radioactivity losses in the metal

screens were rather low (~2%) for moderate aerosol concentrations, i.e., $N \geq 4 \times 10^3$ cm^{-3}. The radioactivity losses for $N \leq 2 \times 10^3$ cm^{-3} (i.e., July 15, 16 and 22/87) could not be determined, unfortunately, because no reference open filter samples were concurrently taken with battery screen measurements. In spite of this, the ratios $\Sigma S/F$ suggest significantly higher radioactivity losses at low aerosol concentrations than at higher concentrations, as expected.

The forward to backward ratio, F/B, for different screen sizes, and aerosol concentrations, N, are shown in Table 6. The tabulated values show that within the aerosol concentration range 6×10^3 to 1.6×10^4 cm^{-3}, the values for the ratio F/B were not dramatically different for the four screen sizes used. The values for F/B decreased with increasing screen size from ~1.88 for screen No. 40 to ~1.10 for screen No. 500. The data in Table 6 were obtained as follows. An overall average value for F/B, i.e., $\overline{(F/B)}$, and the corresponding standard deviation for F/B, SD, were calculated for each screen. Values for F/B which fell outside the range $\overline{(F/B)} \pm 2$ SD were deleted.

It should be noted that the aerosol size distribution investigated in this experiment was polydispersed (see Figures 1 to 5) and, therefore, the F/B ratio is an unknown function of the mesh size and the size of the particles. The reader should bear in mind that the higher the mesh size the more likely it is for the particle to be 'trapped' at the front of the screen (5), whereas the likelihood of the particle to pass through the front of the screen and be 'trapped' at the backside of the screen increases with increasing particle size. A more detailed analysis of this problem will be dealt with in a forthcoming paper.

Figures 1 and 2 show particle concentration, and particle volume size distribution for the aerosol cloud (N ~2×10^3 cm^{-3}) in the RTTF without

external aerosol injection (Figure 1) and when NaCl aerosols were injected in the RTTF (Figure 2). Also shown in the Figures are cumulative particle number (%) versus particle size. Some size (and volume) spectral difference can be observed between these two aerosol coulds. The particle size geometric mean for the aerosol clouds was ~0.092 μm.

Figures 3 to 5 show $dA/Ad(\log D_p)$ versus D_p for three different experiments. In these Figures, A represents the activity of the screen, i.e., ^{212}Pb, ^{212}Bi, or WL(Tn), and D_p represents the size (diameter) of the particle. Calculations were conducted using the Twomey method (7).

Figure 3 shows that for the higher aerosol concentration, the size of the radioactive particles was above 0.06 μm (60 mm). This value is not in disagreement with the size of the aerosol cloud (geometric mean ~0.092 μm (90 mm)). The radioactive aerosol size distribution shown in Figure 3 is typical of at least 10 similar sets of data.

Figure 4 shows that even at aerosol concentrations below ~6 x 10^3 cm^{-3} there is no indication of radioactive particles smaller than that of the aerosol cloud.

Figure 5 suggests that at aerosol concentrations below 2x10^3 cm^{-3}, a low size radioactive particle component is present. Because it is very unlikely that the geometric standard deviation of the aerosol cloud spans over three orders of magnitude, the data of Figure 5 provide evidence, although of a speculative nature, that the radioactive particles have undergone some growth.

It is clear from the data presented here that:

1. Further experimentation should be conducted at lower aerosol concentrations: i.e., $N \ll 2.0 \times 10^3$ cm^{-3}; and
2. The array of metal wire screens (i.e., No. 40, 80, 250 and 500) is not the most suitable one for size distribution analysis purposes in the small

particle size range as that corresponding to the 'unattached' thoron progeny fraction.

Calculation shows that best particle size resolution would be obtained if essentially all screens were of the same high mesh size. Hence, in view of our preliminary results, it is suggested that the next series of experiments should be performed using screen sets of the following mesh sizes: 500, 635, 635, 635.

REFERENCES

1. Chamberlain, A.C. and Dyson, E.D., "The dose to the trachea and bronchi from the decay products of radon and thoron": Brit J Radiol, vol 29, pp 317-325, 1956.

2. Sinclair, D., George, A.C. and Knutson, E.O., "Application of diffusion batteries to measurement of submicron radioactive aerosols": In, Airborne Radioactivity, T. Shaw, (Ed.), American Nuclear Society, La Grange Park, IL, pp 103-114: 1978.

3. Goldstein, S.D. and Hopke, P.K., "Environmental neutralization of Polonium-218": Envir Sci Technol, vol. 19, pp 146-150, 1985.

4. Knutson, E.O., George, A.C., Knuth, R.H. and Koh, B.R., "Measurement of radon daughter particle size": Rad Prot Dos, vol. 7, pp 121-125, 1984.

5. Holub, R.F. and Knutson, E.O., "Measurement of ^{218}Po diffusion coefficient spectra using multiple wire screens": In: Radon and Its Decay Products, ACS Symp. Series No. 331, pp. 340-356., P.K. Hopke (Ed.), American Chemical Society, Washington, D.C., 1987.

6. Bigu, J. and Grenier, M.G., "Thoron daughter Working Level measurements by one and two gross alpha-count methods": Nucl Instrum and Methods in Phys Research, vol. 225, pp. 385-398, 1984.

7. Twomey, S., "Comparison of constrained linear inversion and an iterative

non-linear algorithm applied to the indirect estimation of the particle size distribution": J Comp Phys. vol. 18. pp 188-200. 1975.

Table 1 - Screen characteristics

Mesh No. (in^{-1})	Wire Diameter (cm)	Measured Thickness (cm)	Mass per Unit Area g/cm^2	Solid Fraction x*
40	0.0229	0.0520	0.121	0.298
80	0.0140	0.0296	0.075	0.319
250	0.0041	0.0090	-	0.299
500	0.0025	0.0060	-	0.365

*The screen solid fraction, x, is defined as the ratio of the volume of the solid to the total volume of the screen.

Table 2 - Average thoron progeny and aerosol conditions in the RTTF

Date	$[^{212}Pb]$ pCi/L	$[^{212}Bi]$ pCi/L	$\frac{[^{212}Bi]}{[^{212}Pb]}$	WL(Tn)	N cm^{-3}	Aerosol G.M.. μm
July 15/87	3.73	1.45	0.39	0.48	-	-
July 16/87	3.94	1.72	0.44	0.51	$1.9x10^3$	-
July 17/87	60.77	24.65	0.41	7.80	$9.0x10^3$	-
July 20/87	96.23	44.50	0.46	12.42	$1.15x10^4$	-
July 21/87	91.21	37.79	0.41	11.71	$1.17x10^4$	-
July 22/87	3.77	1.96	0.52	0.49	$\sim 2.2x10^3$	-
July 30/87	87.78	39.78	0.45	11.32	$1.05x10^4$	-
July 31/87	60.11	23.83	~0.40	7.71	$8.4x10^4$	-
Aug. 4/87	102.11	48.04	0.47	13.12	$1.35x10^4$	-
Aug. 5/87	130.68	63.17	0.48	16.90	$1.50x10^4$	-
Aug. 7/87	110.18	51.25	0.46	14.22	$1.6x10^4$	-
Aug. 10/87	113.00	55.17	0.49	14.62	$\sim 1.5x10^4$	-
Aug. 11/87	88.69	43.96	0.49	11.48	$\sim 1.2x10^4$	-
Aug. 14/87	91.28	40.85	0.45	11.76	$1.45x10^4$	-
Aug. 18/87	73.53	30.35	0.41	9.44	$1.05x10^4$	-
Aug. 20/87	74.62	30.69	0.41	9.58	$1.02X10^4$	-
Aug. 25/87	94.50	38.65	0.41	12.13	$1.07x10^4$	-
Aug. 26/87	80.92	35.98	0.44	10.42	$9.5x10^3$	-
Sept. 1/87	83.32	37.75	0.45	10.74	$\sim 7.5x10^3$	0.115
Sept. 2/87	77.20	33.15	0.43	9.93	$6.9x10^3$	0.118
Sept. 3/87	70.98	31.23	0.44	9.14	$4.4x10^3$	0.084
Sept. 4/87	80.25	38.37	0.48	10.37	$6.7x10^3$	0.089
Sept. 9/87	91.33	44.85	0.49	11.82	$5.6x10^3$	0.092
Sept. 11/87	7.27	3.81	0.52	0.94	$2.0x10^3$	0.089

Notes: N stands for aerosol concentration. G.M. is used to denote geometric mean. The square brackets indicate activity concentration.

Table 3 - Thoron progeny losses on wire screens

Date	Wire Mesh No.	$[^{212}Pb]$ (pCi/L)	$[^{212}Bi]$ (pCi/L)	WL(Tn)	$(\Sigma S/F)_1$	$(\Sigma S/F)_2$	$(\Sigma S/F)_3$
July 15/87	500	0.416	0.049	0.052	0.166	0.060	0.161
	250	0.121	0.014	0.015			
	80	0.050	0.010	0.006			
	40	0.030	0.014	0.004			
	Back filter	3.726	1.448	0.477			
July 16/87	500	0.390	0.156	0.050	0.145	0.149	0.146
	250	0.141	0.036	0.018			
	80	0.026	0.034	0.004			
	40	0.014	0.028	0.002			
	Back filter	3.940	1.708	0.507			
July 17/87	500	0.350	0.139	0.045	0.011	0.008	0.011
	250	0.243	0.057	0.031			
	80	0.070	0.002	0.009			
	40	0.039	0.001	0.005			
	Back filter	60.98	24.72	7.83			
July 20/87	500	1.028	0.441	0.132	0.014	0.015	0.014
	250	0.181	0.146	0.024			
	80	0.110	0.052	0.014			
	40	0.048	0.049	0.007			
	Back filter	95.56	44.65	12.46			
July 21/87	500	0.695	0.174	0.088	0.011	0.009	0.011
	250	0.229	0.118	0.029			
	80	0.056	0.013	0.007			
	40	0.038	0.024	0.005			
	Back filter	91.52	37.9	11.76			
July 22/87	500	0.358	0.146	0.046	0.147	0.114	0.147
	250	0.105	0.062	0.014			
	80	0.054	0.006	0.007			
	40	0.037	0.009	0.005			
	Back filter	3.771	1.959	0.489			

Notes: a) $\Sigma S/F$ indicates the sum of activities on the screens divided by the activity on the back filter. The indices 1, 2 and 3 refer to ^{212}Pb, ^{212}Bi and WL(Tn), respectively.

b) Experiments were performed in the forward configuration, i.e., forward exposure and forward measurement.

Table 4 - Thoron progeny losses on wire screens

Date	Wire Mesh No.	[^{212}Pb] (pCi/L)	[^{212}Bi] (pCi/L)	WL(Tn)	$(\Sigma S/F)_1$	$(\Sigma S/F)_2$	$(\Sigma S/F)_3$
July 30/87	40	0.096	0.014	0.012	0.014	0.011	0.014
	80	0.141	0.057	0.018			
	250	0.423	0.116	0.054			
	500	0.664	0.256	0.085			
	Back filter	94.33	40.59	12.14			
July 30/87	40	0.064	0.048	0.008	0.011	0.012	0.011
	80	0.112	0.058	0.015			
	250	0.189	0.100	0.025			
	500	0.696	0.314	0.090			
	Back filter	93.96	44.43	12.14			
July 31/87	40	0.068	0.011	0.008	0.010	0.012	0.010
	80	0.058	0.053	0.008			
	250	0.176	0.073	0.023			
	500	0.329	0.161	0.043			
	Back filter	64.31	25.18	8.24			
July 31/87	40	0.053	-	0.007			
	80	0.059	0.021	0.008	0.011	0.009	0.011
	250	0.217	0.062	0.027			
	500	0.374	0.278	0.050			
	Back filter	64.18	41.44	8.24			
Aug. 4/87	40	0.115	0.033	0.015	0.015	0.013	0.015
	80	0.154	0.044	0.019			
	250	0.359	0.097	0.045			
	500	1.127	0.384	0.144			
	Back filter	117.62	44.23	15.05			
Aug. 4/87	40	0.119	0.049	0.015	0.012	0.011	0.012
	80	0.109	0.067	0.014			
	250	0.380	0.162	0.049			
	500	0.813	0.243	0.103			
	Back filter	116.7	48.99	15.00			
Aug. 5/87	40	0.103	0.046	0.013	0.011	0.011	0.011
	80	0.193	0.072	0.025			
	250	0.390	0.189	0.050			
	500	0.673	0.369	0.088			
	Back filter	125.68	61.44	16.26			

Cont. overleaf

Date	Wire Mesh No.	[^{212}Pb] (pCi/L)	[^{212}Bi] (pCi/L)	WL(Tn)	$(\Sigma S/F)_1$	$(\Sigma S/F)_2$	$(\Sigma S/F)_3$
Aug. 5/87	40	0.074	0.057	0.010	0.012	0.013	0.012
	80	0.118	0.080	0.016			
	250	0.430	0.166	0.055			
	500	0.893	0.509	0.117			
	Back filter	125.82	60.15	16.26			

Notes: a) $\Sigma S/F$ indicates the sum of the activities on the screens divided by the activity on the back filter. The indices 1. 2 and 3 refer to ^{212}Pb. ^{212}Bi and WL(Tn). respectively.

b) Experiments were performed in the forward configuration. i.e.. forward exposure and forward measurement or backward exposure and backward measurement.

Table 5 - Thoron progeny losses on wire screens

Date	Wire Mesh No.	[^{212}Pb] (pCi/L)	[^{212}Bi] (pCi/L)	WL(Tn)	$(\Sigma S/F)_1$	$(\Sigma S/F)_2$	$(\Sigma S/F)_3$
Aug. 7/87	40	0.053	0.049	0.007	0.012	0.014	0.012
	80	0.135	0.074	0.018			
	250	0.467	0.193	0.060			
	500	0.745	0.439	0.097			
	Back filter	116.93	52.97	15.075			
Aug. 7/87	40	0.030	0.027	0.004	0.007	0.011	0.007
	80	0.065	0.045	0.009			
	250	0.100	0.135	0.014			
	500	0.621	0.386	0.081			
	Back filter	116.67	55.50	15.076	(0.019)	(0.025)	(0.019)
Aug. 10/87	40	0.122	0.092	0.016	0.012	0.011	0.012
	80	0.201	0.003	0.024			
	250	0.384	0.130	0.049			
	500	0.649	0.368	0.085			
	Back filter	114.23	54.89	14.77			
Aug. 10/87	40	0.010	0.024	0.002	0.009	0.008	0.009
	80	0.053	0.053	0.007			
	250	0.186	0.123	0.024			
	500	0.829	0.244	0.105			
	Back filter	114.06	56.53	14.77	(0.021)	(0.019)	(0.021)
Aug. 11/87	40	0.046	0.047	0.006	0.015	0.016	0.015
	80	0.153	0.071	0.020			
	250	0.414	0.210	0.054			
	500	0.712	0.337	0.092			
	Back filter	89.73	42.0	11.59			
Aug. 11/87	40	0.060	0.015	0.008	0.011	0.008	0.011
	80	0.079	0.019	0.010			
	250	0.159	0.048	0.020			
	500	0.712	0.261	0.091			
	Back filter	89.91	43.66	11.63	(0.026)	(0.024)	(0.026)
Aug. 14/87	40	0.072	0.036	0.009	0.011	0.012	0.011
	80	0.098	0.075	0.013			
	250	0.289	0.107	0.037			
	500	0.587	0.295	0.076			
	Back filter	91.55	41.38	11.80			
Aug. 14/87	40	0.018	0.017	0.002	0.008	0.010	0.008
	80	0.061	0.031	0.008			
	250	0.134	0.089	0.018			
	500	0.523	0.254	0.068			
	Back filter	91.63	40.58	11.80	(0.019)	(0.022)	(0.019)

Cont. overleaf

Date	Wire Mesh No.	$[^{212}Pb]$ (pCi/L)	$[^{212}Bi]$ (pCi/L)	WL(Tn)	$(\Sigma S/F)_1$	$(\Sigma S/F)_2$	$(\Sigma S/F)_3$
Aug. 18/87	40	0.039	0.051	0.005	0.013	0.015	0.013
	80	0.097	0.074	0.013			
	250	0.348	0.068	0.044			
	500	0.521	0.256	0.067			
	Back filter	75.04	30.6	9.63			
Aug. 18/87	40	0.075	0.004	0.009	0.011	0.008	0.011
	80	0.117	-	0.014			
	250	0.087	0.056	0.011			
	500	0.549	0.192	0.070			
	Back filter	75.01	31.27	9.64	(0.024)	(0.023)	(0.024)
Aug. 20/87	40	0.035	0.038	0.005	0.010	0.012	0.010
	80	0.090	0.033	0.011			
	250	0.152	0.069	0.020			
	500	0.476	0.209	0.061			
	Back filter	74.80	29.98	9.59			
Aug. 20/87	40	0.015	0.009	0.002	0.008	0.007	0.008
	80	0.051	0.003	0.006			
	250	0.186	0.035	0.023			
	500	0.343	0.186	0.045			
	Back filter	74.65	31.33	9.59	(0.018)	(0.019)	(0.018)
Aug. 25/87	40	0.068	0.048	0.009	0.014	0.013	0.014
	80	0.110	0.043	0.014			
	250	0.413	0.138	0.053			
	500	0.801	0.318	0.103			
	Back filter	95.84	42.39	12.34			
Aug. 25/87	40	0.039	0.025	0.005	0.009	0.010	0.009
	80	0.084	0.001	0.010			
	250	0.170	0.046	0.022			
	500	0.554	0.282	0.072			
	Back filter	96.48	36.13	12.34	(0.023)	(0.023)	(0.023)
Aug. 26/87	40	0.073	0.040	0.010	0.009	0.015	0.009
	80	0.089	0.049	0.012			
	250	0.134	0.165	0.019			
	500	0.480	0.304	0.063			
	Back filter	84.67	36.31	10.89			
Aug. 26/87	40	0.003	0.032	0.001	0.010	0.008	0.010
	80	0.066	0.017	0.008			
	250	0.154	0.082	0.020			
	500	0.623	0.179	0.079			
	Back filter	84.43	38.75	10.89	(0.019)	(0.023)	(0.019)

Cont. overleaf

Date	Wire Mesh No.	$[^{212}Pb]$ (pCi/L)	$[^{212}Bi]$ (pCi/L)	WL(Tn)	$(\Sigma S/F)_1$	$(\Sigma S/F)_2$	$(\Sigma S/F)_3$
Sept. 1/87	40	0.129	0.036	0.016	0.014	0.010	0.013
	80	0.125	0.023	0.016			
	250	0.339	0.116	0.043			
	500	0.578	0.199	0.074			
	Back filter	85.14	37.36	10.96			
Sept. 1/87	40	0.054	0.015	0.007	0.009	0.008	0.009
	80	0.059	0.020	0.008			
	250	0.156	0.081	0.020			
	500	0.507	0.222	0.065			
	Back filter	84.91	39.62	10.96	(0.023)	(0.009)	(0.022)
Sept. 2/87	40	0.088	0.045	0.011	0.011	0.012	0.011
	80	0.124	0.054	0.016			
	250	0.232	0.084	0.030			
	500	0.421	0.213	0.055			
	Back filter	78.31	32.89	10.06			
Sept. 2/87	40	0.037	0.024	0.005	0.009	0.010	0.009
	80	0.089	0.014	0.011			
	250	0.198	0.074	0.025			
	500	0.404	0.237	0.053			
	Back filter	78.17	34.26	10.06	(0.020)	(0.022)	(0.020)
Sept. 3/87	40	0.101	0.048	0.013	0.012	0.013	0.012
	80	0.098	0.070	0.013			
	250	0.237	0.105	0.031			
	500	0.445	0.196	0.057			
	Back filter	71.44	31.73	9.20			
Sept. 3/87	40	0.050	0.011	0.006	0.008	0.005	0.008
	80	0.103	0.002	0.013			
	250	0.140	0.042	0.018			
	500	0.291	0.107	0.037			
	Back filter	71.50	31.16	9.20	(0.020)	(0.018)	(0.020)
Sept. 4/87	40	0.108	0.039	0.014	0.013	0.018	0.013
	80	0.118	0.076	0.015			
	250	0.275	0.205	0.037			
	500	0.594	0.392	0.078			
	Back filter	84.02	39.51	10.85			
Sept. 4/87	40	0.045	0.026	0.006	0.009	0.010	0.009
	80	0.049	0.055	0.007			
	250	0.149	0.074	0.019			
	500	0.511	0.234	0.066			
	Back filter	83.90	40.69	10.85	(0.022)	(0.028)	(0.022)

Cont. overleaf

Date	Wire Mesh No.	$[^{212}Pb]$ (pCi/L)	$[^{212}Bi]$ (pCi/L)	WL(Tn)	$(\Sigma S/F)_1$	$(\Sigma S/F)_2$	$(\Sigma S/F)_3$
Sept. 9/87	40	0.140	0.093	0.018	0.014	0.016	0.014
	80	0.174	0.054	0.022			
	250	0.407	0.172	0.052			
	500	0.611	0.403	0.080			
	Back filter	92.89	46.22	12.03			
Sept. 9/87	40	0.065	0.003	0.008	0.009	0.009	0.009
	80	0.070	0.060	0.009			
	250	0.214	0.094	0.028			
	500	0.488	0.266	0.064			
	Back filter	93.01	45.06	12.03	(0.023)	(0.025)	(0.023)
Sept. 10/87	40	0.073	0.061	0.010	0.091	0.109	0.092
	80	0.153	0.052	0.020			
	250	0.168	0.137	0.022			
	500	0.332	0.178	0.043			
	Back filter	7.931	3.920	1.027			
Sept. 10/87	40	0	0.015	0	0.048	0.055	0.049
	80	0.048	0.029	0.006			
	250	0.121	0.058	0.016			
	500	0.210	0.134	0.028			
	Back filter	7.897	4.318	1.028	(0.139)	(0.164)	(0.141)

Notes: a) $\Sigma S/F$ indicates the sum of the activities on the screens divided by the activity on the back filter. The indices 1, 2 and 3 refer to ^{212}Pb, ^{212}Bi and WL(Tn), respectively.

b) The numbers in round brackets represent the 'total' ratio $\Sigma S/F$ where ΣS is given by the (total) activity on the screens measured according to the forward and backward configurations and added together.

c) The first and second sets of numbers for each date represent measurements made according to the forward and backward configurations, respectively.

Table 6 - Thoron progeny forward to backward ratios for several wire screens

Date	Wire Mesh No.	N±SD cm^{-3}	F/B±SD	Σ(F/B)/n ±SD	Total No. of Measurements n
Aug. 7/87	40	15860±498	1.581±0.459	1.876±0.550	36
Aug. 11/87	40	12150±409	1.767±0.690		
Aug. 14/87	40	14820±205	2.307±0.488		
Aug. 18/87	40	10467±372	1.671±0.817		
Aug. 20/87	40	10200±0	1.619±0.916		
Aug. 25/87	40	10750±333	1.900±0.117		
Aug. 26/87	40	9567±625	2.085±0.565		
Sept. 1/87	40	7450±383	2.102±0.439		
Sept. 2/87	40	6917±98	2.121±0.204		
Aug. 7/87	80	15860±498	1.714±0.503	1.803±0.499	44
Aug. 10/87	80	14683±214	1.659±0.615		
Aug. 11/87	80	12150±409	1.916±0.635		
Aug. 14/87	80	14820±205	1.761±0.327		
Aug. 18/87	80	10467±372	1.540±0.506		
Aug. 20/87	80	10200±0	1.797±0.451		
Aug. 25/87	80	10750±333	1.767±0.913		
Aug. 26/87	80	9567±625	2.070±0.477		
Sept. 1/87	80	7450±383	1.884±0.333		
Sept. 2/87	80	6917±98	2.053±0.589		
Aug. 7/87	250	15860±498	2.393±0.337	1.791±0.582	44
Aug. 10/87	250	14683±214	1.439±0.331		
Aug. 11/87	250	12150±409	2.549±0.392		
Aug. 14/87	250	14820±205	1.671±0.240		
Aug. 18/87	250	10467±372	2.039±0.242		
Aug. 20/87	250	10200±0	1.164±0.215		
Aug. 25/87	250	10750±333	2.828±0.261		
Aug. 26/87	250	9567±625	1.545±0.301		
Sept. 1/87	250	7450±383	1.898±0.194		
Sept. 2/87	250	6917±98	1.224±0.097		
Aug. 7/87	500	15800±498	1.210±0.049	1.097±0.145	54
Aug. 10/87	500	14683±214	1.072±0.137		
Aug. 11/87	500	12150±409	1.056±0.135		
Aug. 14/87	500	14820±205	1.141±0.115		
Aug. 18/87	500	10467±372	1.039±0.157		
Aug. 20/87	500	10200±0	1.169±0.189		
Aug. 25/87	500	10750±333	1.124±0.160		
Aug. 26/87	500	9567±625	1.129±0.192		
Sept. 1/87	500	7450±383	1.027±0.055		
Sept. 2/87	500	6917±98	0.935±0.059		

Notes: a) SD stands for standard deviation.
b) n differs for different wire mesh nos. because some data were not included in the calculations on account of poor statistics of counting.

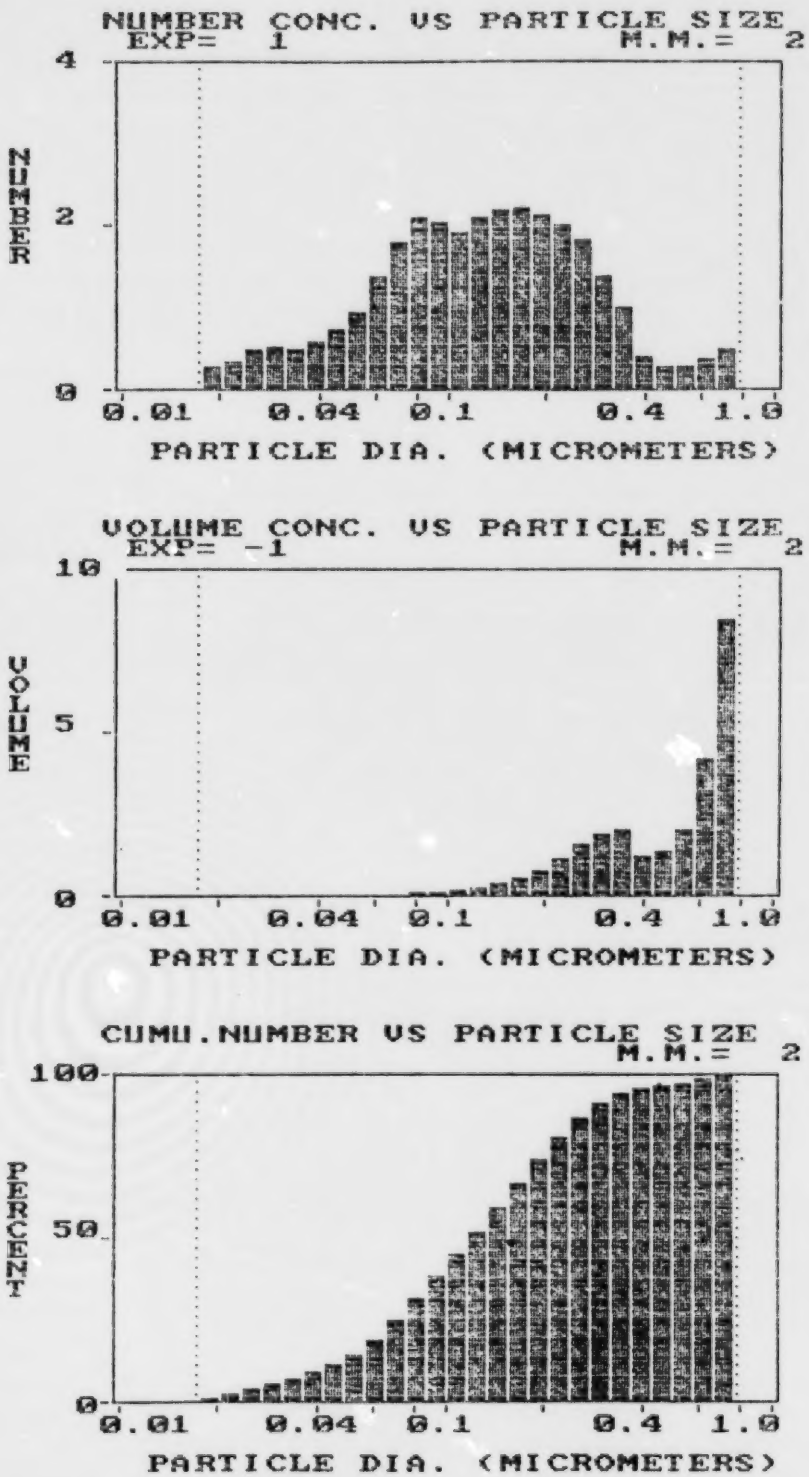

Fig. 1 - Size distributions (aerosol concentration and particle volume) corresponding to the aerosol cloud in the RTTF. Also shown is the cumulative particle concentration versus particle size. No external aerosol injection.

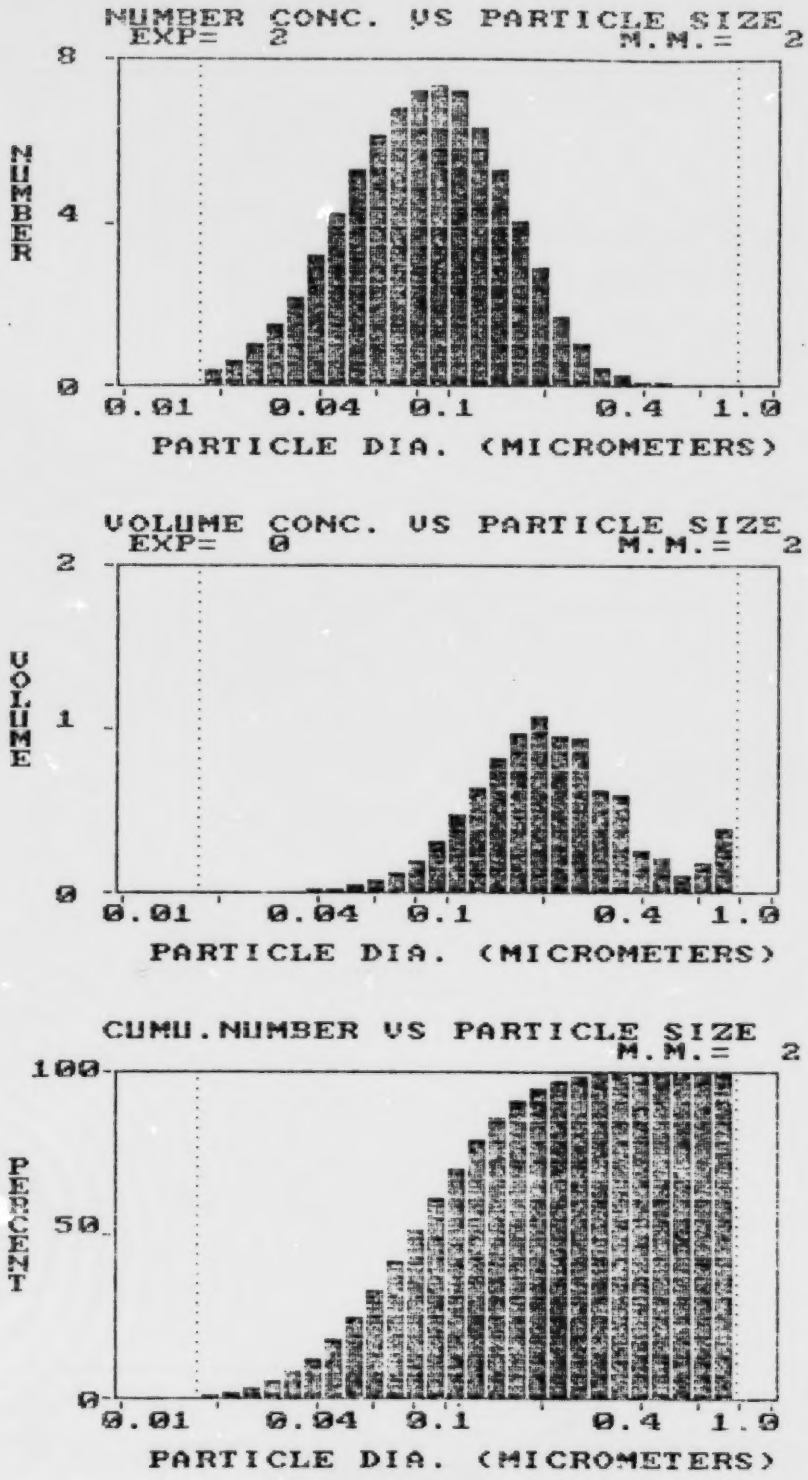

Fig. 2 - Size distributions (aerosol concentration and particle volume) corresponding to the aerosol cloud (NaCl) in the RTTF. Also shown is the cumulative particle concentration versus particle size.

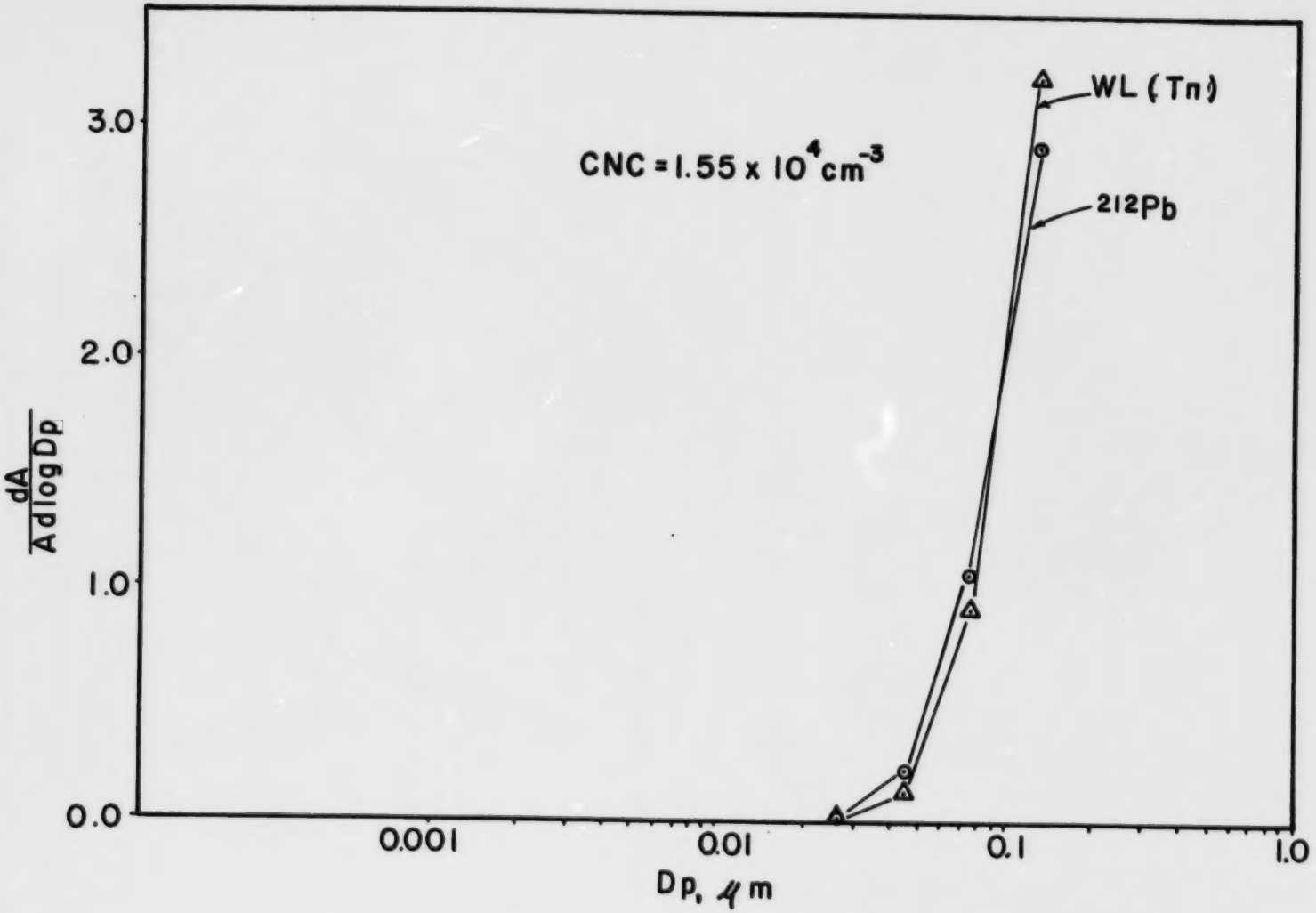

Fig. 3 - $dA/AdlogD_p$ versus particle size for WL(Tn) and ^{212}Pb (aerosol concentration 1.55×10^4 cm^{-3}).

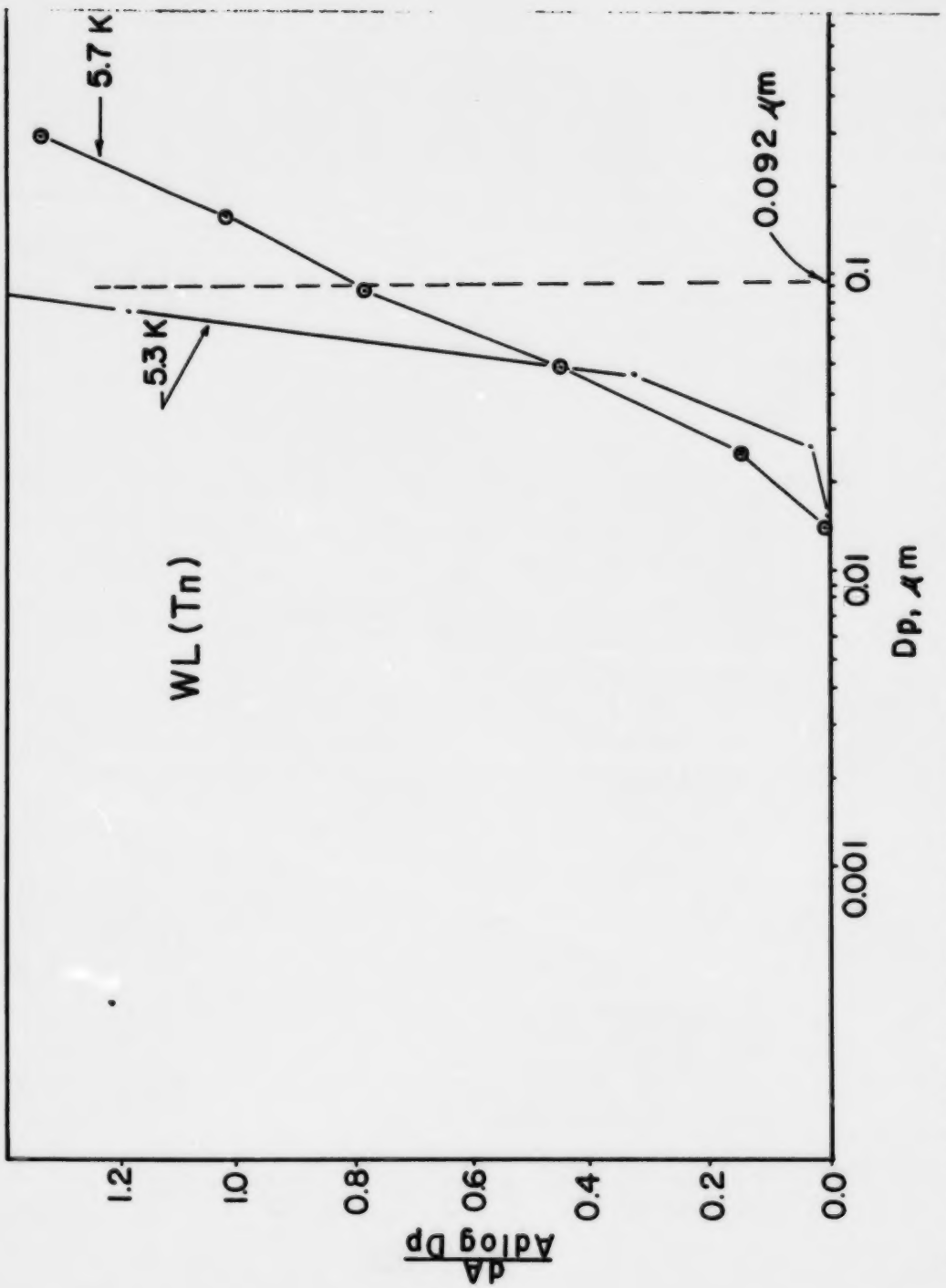

Fig. 4 - $dA/d\log D_p$ versus particle size for WL(Tn) corresponding to two different experiments at low aerosol concentration conditions. (Note: K is used to indicate 10^3 cm^{-3}.)

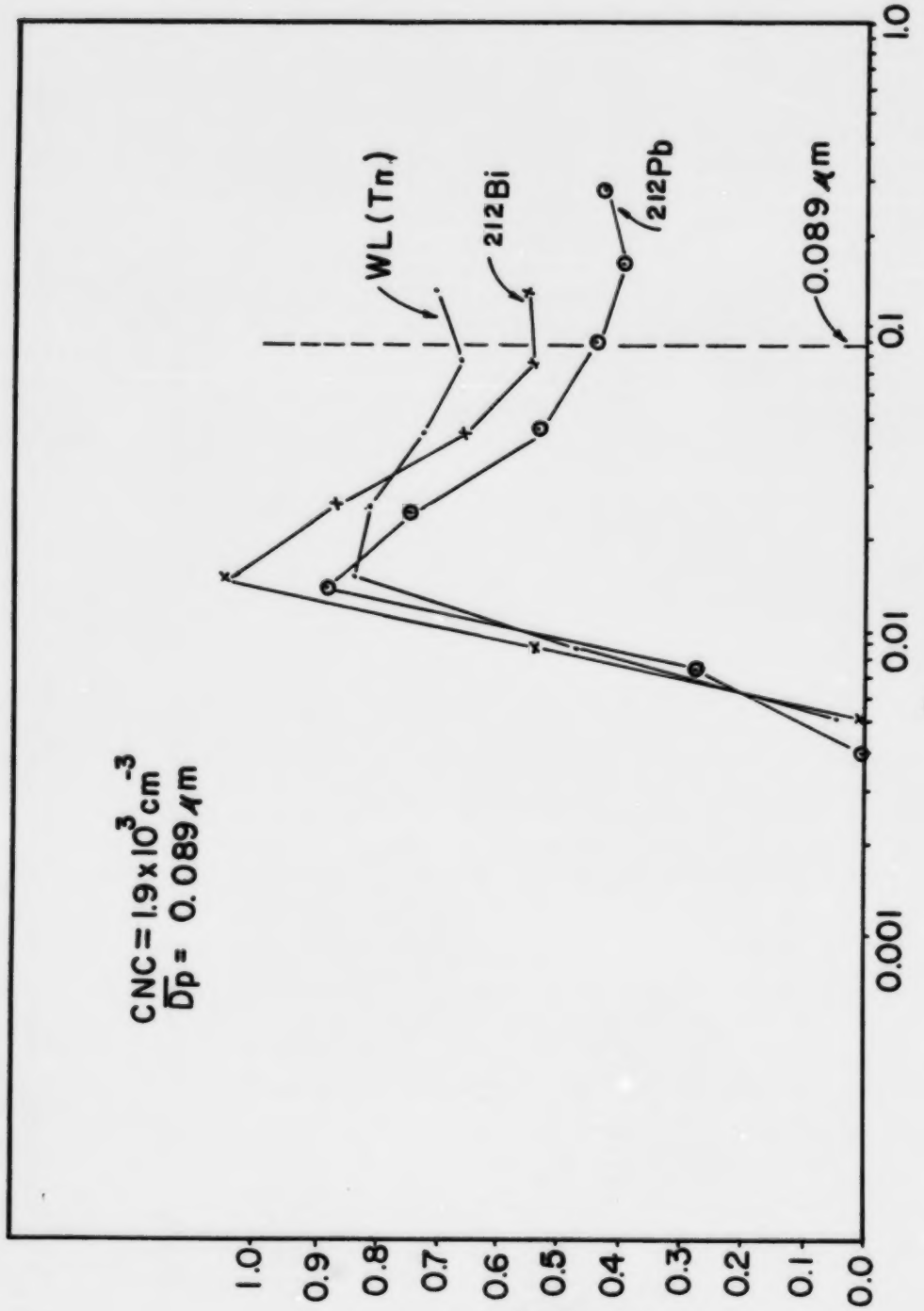

Fig. 5 - $dA/d\log D_p$ versus particle size for ^{212}Bi, ^{212}Pb and $WL_{(Tn)}$ at low aerosol concentration conditions (1.9×10^3 cm^{-3}).